NASA/TM—2002-211474 AIAA–2002–3632

Unsteady Ejector Performance: An Experimental Investigation Using a Resonance Tube Driver

Jack Wilson
QSS Group, Inc., Cleveland, Ohio

Daniel E. Paxson
Glenn Research Center, Cleveland, Ohio

July 2002

The NASA STI Program Office . . . in Profile

Since its founding, NASA has been dedicated to the advancement of aeronautics and space science. The NASA Scientific and Technical Information (STI) Program Office plays a key part in helping NASA maintain this important role.

The NASA STI Program Office is operated by Langley Research Center, the Lead Center for NASA's scientific and technical information. The NASA STI Program Office provides access to the NASA STI Database, the largest collection of aeronautical and space science STI in the world. The Program Office is also NASA's institutional mechanism for disseminating the results of its research and development activities. These results are published by NASA in the NASA STI Report Series, which includes the following report types:

- TECHNICAL PUBLICATION. Reports of completed research or a major significant phase of research that present the results of NASA programs and include extensive data or theoretical analysis. Includes compilations of significant scientific and technical data and information deemed to be of continuing reference value. NASA's counterpart of peer-reviewed formal professional papers but has less stringent limitations on manuscript length and extent of graphic presentations.

- TECHNICAL MEMORANDUM. Scientific and technical findings that are preliminary or of specialized interest, e.g., quick release reports, working papers, and bibliographies that contain minimal annotation. Does not contain extensive analysis.

- CONTRACTOR REPORT. Scientific and technical findings by NASA-sponsored contractors and grantees.

- CONFERENCE PUBLICATION. Collected papers from scientific and technical conferences, symposia, seminars, or other meetings sponsored or cosponsored by NASA.

- SPECIAL PUBLICATION. Scientific, technical, or historical information from NASA programs, projects, and missions, often concerned with subjects having substantial public interest.

- TECHNICAL TRANSLATION. English-language translations of foreign scientific and technical material pertinent to NASA's mission.

Specialized services that complement the STI Program Office's diverse offerings include creating custom thesauri, building customized data bases, organizing and publishing research results . . . even providing videos.

For more information about the NASA STI Program Office, see the following:

- Access the NASA STI Program Home Page at ***http://www.sti.nasa.gov***

- E-mail your question via the Internet to help@sti.nasa.gov

- Fax your question to the NASA Access Help Desk at 301–621–0134

- Telephone the NASA Access Help Desk at 301–621–0390

- Write to:
  NASA Access Help Desk
  NASA Center for AeroSpace Information
  7121 Standard Drive
  Hanover, MD 21076

NASA/TM—2002-211474 AIAA–2002–3632

Unsteady Ejector Performance: An Experimental Investigation Using a Resonance Tube Driver

Jack Wilson
QSS Group, Inc., Cleveland, Ohio

Daniel E. Paxson
Glenn Research Center, Cleveland, Ohio

Prepared for the
38th Joint Propulsion Conference and Exhibit
cosponsored by AIAA, ASME, SAE, and ASEE
Indianapolis, Indiana, July 7–10, 2002

National Aeronautics and
Space Administration

Glenn Research Center

July 2002

The Aerospace Propulsion and Power Program at NASA Glenn Research Center sponsored this work.

Available from

NASA Center for Aerospace Information
7121 Standard Drive
Hanover, MD 21076

National Technical Information Service
5285 Port Royal Road
Springfield, VA 22100

Available electronically at http://gltrs.grc.nasa.gov/GLTRS

UNSTEADY EJECTOR PERFORMANCE: AN EXPERIMENTAL INVESTIGATION USING A RESONANCE TUBE DRIVER

Jack Wilson*
QSS Group, Inc.
Cleveland, Ohio 44135

Daniel E. Paxson†
National Aeronautics and Space Administration
Glenn Research Center
Cleveland, Ohio 44135

Abstract

A statistically designed experiment to characterize thrust augmentation for unsteady ejectors has been conducted at the NASA Glenn Research Center. The variable parameters included ejector diameter, length, and nose radius. The pulsed jet driving the ejectors was produced by a shrouded resonance (or Hartmann-Sprenger) tube. In contrast to steady ejectors, an optimum ejector diameter was found, which coincided with the diameter of the vortex ring created at the pulsed jet exit. Measurements of ejector exit velocity using a hot-wire permitted evaluation of the mass augmentation ratio, which was found to correlate to thrust augmentation following a formula derived for steady ejectors.

Introduction

Currently, efforts are underway to explore the use of pulsed detonation engines (PDE) for aerospace propulsion. Technical issues involved include integration, noise, and thrust to weight ratio. Adding an ejector to a PDE may enhance thrust, and reduce noise. The ejector will then be driven by a pulsating flow. Past studies of unsteady ejectors[1–3] have shown that thrust augmentation ratios up to about 2 have been achieved, but with conflicting results regarding the parameter settings to achieve this value. For example, both Lockwood,[1] and Binder and Didelle,[2] plot thrust augmentation ratio against ejector length, L, divided by ejector diameter, D. Lockwood found a maximum augmentation ratio at $L/D \approx 1.5$, whereas Binder and Didelle found their maximum at $L/D = 9$. This suggests that L/D is not the correct parameter for this correlation, but does show that unsteady ejectors can be quite short. Both Lockwood, and Binder and Didelle, varied ejector length in their experiments, but held ejector diameter constant.

Johnson and Yang[4] reported measurements, together with supporting calculations, of pulsed jet mass entrainment ratios. They did not measure thrust. In the calculations, the assumption was made that the jet acts like a periodically applied piston. The calculation was in good agreement with the experiments. Despite this, theoretical understanding of the flow processes in an unsteady ejector is very limited, and there is no guidance on how to design an unsteady ejector.

The objective of the present study was to perform an experiment to generate information on unsteady ejector performance, with a controlled set of parameter variations. For the study, a resonance, or Hartmann-Sprenger tube[5] was chosen as the source of pulsed air. The output from the resonance tube was directed into a cylindrical shroud, to form the pulsed jet at the exit of the shroud. The resulting pulse had an almost triangular shape (in time) with the rise to the peak somewhat shorter than the decay, similar to a detonation pulse. Johnson and Yang[4] showed that mass entrainment increases significantly as the jet temperature rises. In a companion paper, the results of a study similar to this study are reported, in which a pulsejet was used as the pulsating jet source.[6] Since the pulsejet has a higher temperature, higher values of thrust augmentation were anticipated, and were observed.

Theoretical Considerations

By assuming that the primary (i.e., jet) flow, and the secondary (i.e., entrained by the ejector) flow achieve a uniform velocity, Bertin,[3] and others, have shown that the thrust augmentation, α, (ratio of thrust of jet plus ejector to thrust of the jet alone) achievable with an ejector is related to the entrainment ratio, β, (ratio of entrained mass flow to jet mass flow) by

*Senior Engineering Specialist, Associate Fellow, AIAA.
†Aerospace Engineer, Senior Member, AIAA.

$$\alpha = \sqrt{\eta(1+\beta)} \qquad (1)$$

where η is the efficiency of transfer of kinetic energy from the primary and secondary flows to the exit flow. The above formula is applicable only to a stationary engine. For a moving engine, the augmentation is given by a slightly more complicated formula, showing that it diminishes as speed increases. All values quoted in this work will be for stationary conditions only. In practice, by comparing the experimental results from many workers, Porter and Squyers[7a] have shown that, for steady ejectors, a practical limit appears to be given by

$$\alpha = (1+\beta)^{(\gamma-1)/\gamma} \qquad (2)$$

where γ is the ratio of specific heats. The difficulty in applying this to ejector design is that there does not appear to be a way to relate β to ejector area, at least for unsteady flows. In addition, Porter and Squyers[7b] show that there is a maximum value of thrust augmentation, which depends on the ratio of the jet stagnation to exhaust static pressure ratio, namely

$$\alpha_{max} = 0.9/\sqrt{\xi} \qquad (3)$$

where $\sqrt{\xi}$ is the ratio of the actual jet velocity to the jet exit velocity if it were expanded to a vacuum. From this, lower jet Mach number flows are more likely to produce high values of thrust augmentation.

Johnson and Yang[4] used a one-dimensional method of characteristics calculation to evaluate β for an ejector with a stagnation pressure temporal distribution corresponding to their unsteady experiment. These authors achieved good agreement with measured values of β, but provided no indication of the relationship of β to ejector area. They also concluded from their model that β should increase as the jet temperature increases, a result consistent with their experimental results, which were over a very limited temperature range. This result appears to differ from results with steady ejectors, for which α decreases as temperature increases.[7c] Johnson and Yang also calculated, for square pulses, that β should increase as the pulse width decreases. Using a CFD calculation based on the unsteady code of Paxson,[8] the present authors have found good agreement with Johnson and Yang's calculations of β as a function of pulse width, and confirmed that β increases with temperature.

Pulsed Jet Source

The optimum source of a pulsed jet for the proposed experiment would be a pulsed detonation device. Such devices, particularly with long duration, are not simple to build and operate. In contrast, a resonance, or Hartmann-Sprenger tube,[5] can operate continuously, and generates significant noise. This resonance tube consists of a steady, sonic or supersonic jet, which is blowing into a closed tube. Under certain conditions, a periodic cycle is established in which the jet first fills the tube, then a hammer shock inside the tube empties the tube, deflecting the jet from the tube in the process. When the tube pressure has fallen sufficiently, the cycle can begin again. What was not known at the start of this effort was whether this phenomenon could also produce a directed, pulsed jet. To attempt this, a cylindrical shroud was placed around the tube and jet, to collect the air leaving the tube and direct it out the back of the shroud. Resonance tubes have been shrouded previously,[9] but with acoustic horns, with the objective of amplifying the sound. These acoustic horns were closed at the end where the source is located, and increased in area with distance away from the source. The flow from the horn would therefore be diverging, and the velocity at the exit would be reduced in value from that leaving the source. In order to create a more concentrated flow, a cylindrical shroud was used in the present work. As described below, this shroud did produce a directed, pulsed, flow.

The shrouded tube used is shown in figure 1. A Mach 2 axisymmetric nozzle with a 0.5 inch diameter throat was aligned with a resonance tube 6 inches in length. This was surrounded by a 2 inch diameter shroud. A needle was aligned with the axis of the jet to stimulate oscillations, as demonstrated by Brocher[5]. A supply of air at a pressure of 7.8 atmospheres ensured Mach 2 operation exhausting to the atmosphere. The average mass flow was measured upstream of the nozzle, using an orifice, and was found to be 0.46 lb/sec, at a pulsation frequency of 550 Hz, as well as at steady state.

Design of the Experiment

The unsteady experiments to date in which thrust augmentation was measured for a pulsating jet, namely those of Lockwood[1] and Binder and Didelle,[2] have each shown a peak of thrust augmentation at some value of L/D, with an approximately parabolic distribution of augmentation about that peak. Thus it is appropriate to use a statistical design with a 3 level set of parameters in the experiment. There are many parameters that can affect the performance of an ejector, e.g., ejector length, ejector diameter, distance from jet exit to ejector entrance, ejector geometry, ratio of jet temperature to entrained air temperature, jet frequency, and details of the driving pulse (i.e., pulse amplitude, duration, and temporal distribution, and frequency). By fixing the frequency of the driving jet, having it produce an invariant pulse, and not heating the air supplying the jet, the list is reduced somewhat, although obviously at the cost of not determining the effect of these now fixed parameters. Of the remaining variables, ejector length, diameter and nose radius were chosen as independent parameters. The distance from jet exit to ejector entrance was treated as a dependant parameter, i.e., it was varied for each ejector combination until a maximum value of thrust augmentation was found. A 3 parameter, 3 level Box-Behnken design[10] was chosen for the experiment. The test matrix used is given in Table 1, as runs 1 through 15.

A set of ejectors was built as shown in figure 2(a), consisting of entrance sections, center sections, and a diffusing tail section. At each diameter, three nose sections were made, each of a different nose radius, R, two center sections of different length, and one tail section. By using either no center section, a short center section, or a long one, three different lengths of ejector were obtained, roughly 3, 7.5, and 12.5 inches. Since prior experiments with steady ejectors have shown that thrust augmentation increases with the ratio of exhaust area to jet area,[7d] with values as high as 100 having been used, it appeared that the experiment should include large ejector diameter to jet diameter ratios. Consequently, ratios of ejector throat diameter to jet exit diameter of 1.5, 3, and 4.5 were chosen. Experiments with the ratios 1.5 and 3 soon showed that the optimum augmentation was at a ratio less than 3. Instead of pursuing the experiments with the ratio 4.5 ejectors, a new set at a diameter ratio of 1.1 was made.

Following the initial experiments of the Box-Behnken design, additional runs were made with a set of ejectors of diameter ratio equal to 2 (runs 16 –19 of table 1), and also with additional lengths (runs 20–26 of table 1). Finally, a contoured nozzle, as shown in figure 2(b), with a 3 inch diameter throat, and, initially, a 4 inch diameter exit was built, and used to assess the effect of contouring, and lengths intermediate to those used above (runs 27–32 of table 1).

In these experiments, the objective was measurement of thrust augmentation. However, an ejector also results in mass augmentation, and it is of interest to correlate thrust augmentation and mass augmentation. A hot wire, used to measure velocity in the ejector exit flow provided a means for calculating entrainment ratio. Details are given in subsection 3 of the results section.

Apparatus

The apparatus is shown in figure 3. The resonance tube is mounted vertically, with the jet flowing upwards. The ejector is mounted above the resonance tube, on a sliding mount so that its height is easily adjustable. Above the ejector is a thrust plate, which is 30 inches in diameter. The thrust plate is attached to an Omega load cell model LC601–25, which has a range of ±25 lbs, to provide an electrical thrust signal. Similarly the ejector was attached to another load cell, also a model LC601–25. The signal from both load cells was fed to Agilent model 34401A averaging multimeters. All runs lasted one minute, during which time the voltmeters stored 180 readings, and then displayed the average value. The experimental procedure involved making three tests to read the thrust of the jet without the ejector, followed by a series of tests with the ejector, (two at each setting of jet exit to ejector distance), followed again by three tests reading the thrust of the jet without an ejector. The jet thrust, T_{jet}, defined as the average of the six test readings without the ejector, typically measured 10.00 ± 0.11 lbs. The signal from the ejector load cell corresponds to the additional thrust, ΔT, produced by the ejector. Thus the quantity τ, defined as

$$\tau = 1 + \Delta T/T_{jet} \qquad (4)$$

should be the same as the thrust plate measurement of thrust augmentation, α.

In addition to thrust augmentation, it is desirable to measure mass flow augmentation. For this measurements of the jet mass flow, and the mass flow leaving the ejector are needed. Since the Mach 2 nozzle in the resonance tube is choked, the jet mass flow can be measured upstream of the nozzle, where it will be a steady reading. For this a standard orifice was mounted in the supply line to the jet. The jet flow was measured both as a steady supersonic flow, i.e., with the resonance tube removed, and with the resonance tube in place. The resulting mass flow was indeed identical, with a value of 0.458 ± 0.002 lb/sec. For measuring the mass flow at the exit of the ejector, two techniques were implemented; first, probing the flow with a high frequency pressure transducer (Endevco model 8530C–100), mounted in the hemispherical nose of a cylinder; and second, probing the flow with a Thermal Systems, Inc. model IFA 300 hot-wire, which provided the radial distribution of velocity at the ejector exit.

Experimental Results

Thrust Augmentation

In figure 4 are shown measurements of thrust augmentation, α, versus the jet exit to ejector entrance distance, x, for the 3 inch diameter contoured ejector. The results are typical of all the ejectors: thrust augmentation has a maximum at some distance, which depends mainly on the diameter of the ejector, falling off slowly as distance increases beyond the maximum, but quite rapidly as distance decreases below the maximum. The maximum value of τ, the thrust augmentation derived from the ejector load cell reading, occurs at lower values of x than does α. This may be due to a decrease in the jet thrust when x is small or negative, which is reflected in the measurement of α, but not of τ as defined above. At the maximum of augmentation however, and for larger values of x, both α and τ are in good agreement. In the remainder of this work, the thrust augmentation ascribed to a particular ejector is the maximum value of α.

The measurements of thrust augmentation found in the initial set of Box-Behnken runs are given in table 1, and in figure 5, in which thrust augmentation is plotted against ejector length, L, for each ejector diameter, D, at different values of the nose radius, R. The 90% confidence error bar is shown in the symbol box. The data from a Box-Behnken 3 parameter set can be fitted with a response surface of the form

$$\alpha = b_0 + b_1.L + b_2.D + b_3.R + b_{11}.L^2 + b_{22}.D^2 + b_{33}.R^2 + b_{12}.L.D + b_{13}.L.R + b_{23}.D.R \tag{5}$$

where the values of the constants b_{ii} are determined from the data. This was performed by inserting the data into a computer program,[11] which provides values of the confidence level for each constant. Constants with low confidence level were eliminated, until only terms with levels greater than 90% were retained. The resulting response is

$$\alpha = 0.230 + 9.60.10^{-3}\,L + 0.513.D + 0.3314.R - 1.624.10^{-3}\,L^2 - 6.86.10^{-2}\,D^2 - 0.319\,R^2 + 4.576.10^{-3}\,L.D \tag{6}$$

Although this formula includes R, changes in α due to changes in R for the range of values used are very small, and the changes seen experimentally are statistically insignificant. Sections through this response surface at each value of ejector diameter, D, for R = 0.5, are also plotted on figure 5, showing good agreement with the experimental results. The maximum value of thrust augmentation predicted with this model is 1.389 at L = 8.56, D = 4.0, and R = 0.5. Consequently a new set of 4 inch diameter ejectors was built. Runs 16 through 19 of table 1 were made with this set of 4 inch diameter ejectors. A new response surface for the matrix comprised of runs 1 through 15, and 16 through 19, predicted the optimum ejector to be 3.25 inches in diameter, and 8.9 inches in length, with a maximum value of thrust augmentation of 1.33. Since this is only marginally larger than the thrust augmentation found with the 3 inch diameter ejector, it did not seem worthwhile to build a new set of ejectors of 3.25 inches diameter.

Measurements of thrust augmentation with the same set of ejectors as used here, but with a pulsejet driver,[6] showed maximum thrust augmentation for longer ejectors than was found here. Consequently it was decided to evaluate a longer ejector length by assembling both the center sections together, which resulted in an overall length of about 17 inches. Runs 20 through 26 of table 1 were performed, with the results shown in figure 6, plotted now against ejector length divided by ejector diameter. In figure 6, the data for any one diameter, regardless of nose radius, are fit individually by either a cubic or a quadratic least squares fit, i.e., there was no attempt to create a response surface. Noticeable now is that it appears that there may be a second maximum at longer ejector lengths. Also the optimum ejector length for any diameter is not at a singular value of L/D, but at increasing L/D as the diameter increases. However, the longer lengths did not result in any greater thrust augmentation, and therefore are not of any practical interest.

The possible existence of a second maximum raised the question of whether there might be "fine structure" as a function of length, i.e., that there might be many maxima at lengths intermediate to those used. Further, there is the question of whether a better diffuser, with a more gradual exit angle, would generate more thrust. To address these questions, an existing 4 inch diameter diffuser was modified by inserting balsa wood to create a 3 inch diameter throat, tapering to a 4 inch exit, with an overall length of 10.75 inches. The balsa wood was sanded to shape, then varnished and fine sanded to a smooth surface. The geometry is shown in figure 2(b). Thrust augmentation was measured, and then a portion of the end of the diffuser was removed to shorten the overall length. This was repeated several times (runs 27 through 32 of table 1). The results are shown in figure 7, together with the results from the 3 inch diameter ejector used above. It does not appear that the diffuser made any difference, nor that there is any fine structure.

Finally, the resonance tube was removed, and the steady jet from the Mach 2 nozzle was used to measure thrust augmentation with the 3 inch diameter, 7.4 inch long ejector, which had given the best unsteady thrust augmentation of 1.32. The mass flow through the nozzle was varied from 0.1 lb/sec to 0.46 lb/sec by adjusting the stagnation pressure. Thus it was not a correctly expanded Mach 2 jet, except for the last point. The thrust augmentation was constant at α = 1.12.

Jet Probing

The structure of the unsteady jet itself might be playing some role in the thrust augmentation. In order to explore this, a fast response transducer (Endevco model 8530C–100) was built into the nose of a hemisphere-cylinder body, and inserted into the flow at the same distance from the jet exit as the entrance to the 3 inch diameter, 7.4 inch long, 0.5 inch nose radius ejector at its optimum spacing, i.e., the spacing giving maximum thrust augmentation, which was 3 inches for this ejector. The output from the probe was displayed on an oscilloscope, using dc coupling. The signals, as shown in the upper oscillogram in figure 8(a), with the probe close to the axis of the jet, exhibited a rise in pressure with time, followed by a decay, returning to atmospheric pressure at about half the period of the pulses. After the signal returned to atmospheric, there appeared to be a high frequency oscillation on it, lasting until the next pulse. As the probe was moved radially, away from the jet axis, the value of the peak pressure first increased slightly, then decreased to zero at a radial position equal to about 1.2 times the jet radius. At distances greater than this, a pulse was seen which was a reduction in pressure, with a minimum pressure below atmospheric. The maximum values of the positive pulse signals, and the minimum values of the negative pulse signals are plotted as a function of distance from the jet axis in figure 8(b), as series 1. To explore whether the negative and positive pulses were in phase with one another, a second probe was mounted parallel to the first, both probes were inserted into the flow, and a second series run with both probes. The results are given as series 2 in figure 8(b). In the oscillogram in figure 8(a), the probes were placed so that one probe was reading a positive pulse, and the second was reading a negative pulse. The pulses are exactly in phase. The absolute outer edge of the disturbance, where there is no longer any signal, is at a radial position of 3.2 times the jet radius, or a diameter of 6.4 inches, much larger than the optimum ejector diameter. The optimum ejector diameter actually corresponds to the position of the minimum of the negative pressure signals, i.e., 1.5 times the jet exit diameter.

Initially it was not clear what the pressure signals represented. It was presumed that it would correspond to the stagnation pressure behind a shock wave leaving the shroud, but the signal seemed too low. To examine this, the two-probe arrangement was set up so the probes straddled the jet axis, each equidistant from the probe axis, but with probe number 2 separated axially from probe 1. The objective was to measure the axial velocity of the pulses. Measurements were made at two different axial positions, with the same result: the velocity of the pulse leading edge was 298 ft/sec. This is much too low a velocity to be a shock wave. Experiments with shock waves emerging from tubes[12,13] have shown the existence of a vortex ring traveling behind the shock. From the work of Elder and de Haas,[12] this vortex ring appears to travel at approximately the gas velocity behind the shock, which is consistent with the value measured here, suggesting that the pulse observed might be a vortex ring. The translational velocity of a vortex ring, V_T, is given by[14,15]

$$V_T = \mathbf{\Gamma}/4\pi R_v \{\ln(8R_v/a) - 0.25\} \qquad (7)$$

in which $\mathbf{\Gamma}$ is the circulation, R_v is the vortex ring radius, and a the vortex core radius. The vortex ring radius is the radius at which the velocity is equal to the translational velocity of the vortex ring, i.e., 298 ft/sec for the experimental pulse, if it is a vortex ring. At 298 ft/sec, the stagnation pressure is 1.05 atmospheres, which corresponds to a radius of 1.15 inches in figure 8. The core radius is the radius of the pressure minimum minus the core radius, which is 0.35 inches. The circulation is given by[16]

$$\mathbf{\Gamma} = 0.65 \int U_p(t)^2 dt \qquad (8)$$

in which $U_p(t)$ is the velocity on the centerline, as a function of time. $U_p(t)$ was derived from the centerline pressure trace. Performing the integration lead to $\mathbf{\Gamma}$ = 104 ft^2/sec. Substituting $\mathbf{\Gamma}$ = 104 ft^2/sec, R_v = 0.0958 ft, and R_v/a = 3.29 into the above formula for the vortex ring velocity gave V_T = 260 ft/sec. This is not perfect agreement, but is close enough to indicate that the flow emerging from the resonance tube is a vortex ring.

Gharib et al.[17] define a "formation number," N, as

$$N = \int U_p(t)dt/D_{jet} \qquad (9)$$

where D_{jet} is the nozzle diameter, and show that for $N < 4$, a pulsed flow emerging from a nozzle will transform entirely to a vortex ring. For the resonance tube pulses, $N \sim 2$, giving further confirmation that the flow is a vortex ring.

Mass Flow Augmentation

An initial attempt to measure mass flow augmentation was made by performing a pitot pressure radial traverse of the ejector exit flow, using the 3 inch diameter, 7.4 inch long ejector, with the high frequency pressure transducer used above. The measured pressure traces were remarkably steady in time. An average velocity (in time), U, and density ρ, were calculated at each radial position, r, and integrated to give the total mass flow leaving the ejector, $\dot{m}_{total}$

$$\dot{m}_{total} = \int 2\pi\rho U r dr \quad (10)$$

and also the thrust, T

$$T = \int 2\pi\rho U^2 \, r dr \quad (11)$$

Whilst this procedure gave reasonable values for the total mass flow, the thrust values were significantly lower than the jet thrust, contradicting the thrust plate readings. Consequently, it was decided to make traverses with a hot-wire, which measures the velocity directly. An example of an oscillograph trace of the hot-wire signal, as a function of time, with the hot wire situated on the ejector centerline, is given in figure 9(a). The velocity derived from the hot-wire signal is given in figure 9(b). It will be seen that the oscillogram has rapid fluctuations, which are not picked up in the derived data. This is because the recording device for the hot-wire (a Datamax) was set at too low a frequency. Unfortunately, it was not possible to repeat the measurements with a higher frequency setting. This is probably not a problem for the mass flow value, which only needs an average of velocity in time, so that velocity fluctuations average out. The thrust calculation involves a time average of the square of the velocity, which includes the square of the velocity fluctuations, and so needs an accurate knowledge of the fluctuations.

With the hot-wire, values of the total mass flow were obtained for the 3 inch diameter, 7.4 inch long ejector, and for the 2.2 inch diameter, 7.4 inch long ejector. The results are given in Table 2, expressed as a value of β, in the rows for runs 2 and 8. Thrust augmentation values calculated from the hot-wire signal were 1.25 for run 2, and 0.95 for run 8, which are low.

Discussion of Results

The ultimate objective of ejector research is to understand the mechanism of thrust and mass augmentation, so that predictions of performance can be made, and optimum ejectors designed. There are three major interactions proposed for this mechanism. First is that the unsteady primary pulse acts like a piston which pushes secondary air in front of it, and drags secondary air along behind it. Secondly, shear at the primary-secondary interface drags secondary air into the ejector. Finally, the vortex produced by the unsteady pulse leaving the jet nozzle acts to entrain secondary flow. Shear would appear to be the only interaction for steady flow. Steady ejectors, as noted above, have increasing augmentation as ejector diameter increases. The experiments described here definitely have an optimum diameter, and the thrust augmentation is larger than the steady value seen with the same ejector, indicating a different mechanism.

In Table 1 the measured values of β are used to evaluate the quantity $(1 + \beta)^{(\gamma-1)/\gamma}$, which was shown by Porter and Squyers[7a] to correlate with α for steady ejectors. Remarkably, this also seems to be the case for the present unsteady ejectors (see also ref. 6). Given this, it is possible to use the one dimensional CFD program mentioned above to calculate β as a function of length for a pulse shaped like the measured pulse from the resonance tube, and convert it to α. The result is shown in figure 10, together with the results for the 2.2 inch diameter ejectors, and the 3 inch diameter ejectors. The calculated curve shows two peaks, showing some similarity to the data (although a second peak was not actually observed in the experiment), but is lower in value. It is not clear how to extend this calculation to the 3 inch diameter and larger ejectors, for which higher values of α were seen. Thus the calculation does not agree with the data. Since this calculation corresponds to the piston model, it would appear that the piston interaction is not the entire mechanism, but it may play a partial role. In addition, this calculation is one-dimensional, whereas the measurement of pressure in the jet flow (fig. 8) shows very strong radial variations, which cannot appear in a one-dimensional calculation.

The probing of the jet emerging from the resonance tube has demonstrated that the flow constitutes a strong vortex ring. This vortex ring generates significant sub-atmospheric pressures at a radius of 1.5 inches. This low pressure, acting on the nose of an ejector, will create thrust on the ejector. According to this model, the best ejector, i.e., the one producing the most thrust augmentation, would have about the same radius as the pressure minimum, which is a 3 inch diameter ejector. Smaller, or larger, diameter ejectors would have a higher pressure on the nose, giving reduced thrust. This is in fact what was observed. This model does not explain why there should be an optimum length. This may be clarified, and quantified, by CFD calculations of the flow, and this work is in progress.

Conclusions

A statistical experiment in which ejector length, diameter and nose radius were varied showed that there is an optimum diameter and length giving maximum thrust augmentation for an unsteady ejector. The thrust augmentation was greater for unsteady flow than for steady flow with the same ejector. The ejector with the maximum experimental thrust augmentation was 3 inches diameter, 7.4 inches long, with a 0.5 inch nose radius, for which a thrust augmentation of 1.32 was observed. The ratio of L/D for this ejector is 2.5, intermediate to the results of Lockwood,[1] and Binder and Didelle.[2] The existence of an optimum diameter for an unsteady ejector contrasts with results for steady ejectors, for which thrust augmentation increases monotonically with diameter. Ejector nose radius was shown to be statistically unimportant, but this is in disagreement with other results.[6] Change in the shape of the exit diffuser did not affect the thrust augmentation. Pressure measurements of the flow emerging from the resonance tube showed it to be a vortex ring, with a pressure minimum at a radius of 1.5 inches. This coincides with the diameter of the optimum ejector.

Measurements of mass augmentation were made using a hot-wire, and showed that the correlation of thrust augmentation to mass augmentation derived by Porter and Squyers[7a] for steady flow, also holds for unsteady flow.

This work has served to provide a data base for understanding pulsed ejectors. CFD calculations are in progress to provide details of the flow, and mechanisms involved. This will potentially identify a design methodology.

References

1. Lockwood, R.M. “Interim Summary Report on Investigation of the Process of Energy Transfer from an Intermittent Jet to Secondary Fluid in an Ejector-type Thrust Augmenter,” Hiller Aircraft Report No. ARD–286, March 1961.
2. Binder, G. and Didelle, H, “Improvement of Ejector Thrust Augmentation by Pulsating or Flapping Jets,” Paper E3 of Proc. 2nd Symposium on Jet Pumps & Ejectors and Gas Lift Techniques, Cambridge, England, March 1975.
3. Bertin, J. “Dilution pulsatoire sur réacteur,” Comptes Rendues des Séances de l’Académie des Sciences, Vol. 240, pp. 1855–1857, 1955.
4. Johnson, W.S. and Yang, T. “A Mathematical Model for the Prediction of the Induced Flow in a Pulsejet Ejector with Experimental Verification,” ASME Paper 68–WA/FE–33, 1968.
5. Brocher, E. “Contribution à l’étude des générateurs acoustique à jet d’air,” Acustica, Vol. 32, pp. 227–235, 1975.
6. Paxson, D.E. and Wilson, J. “Unsteady Ejector Performance: An Experimental Investigation using a Pulsejet Driver,” Paper AIAA–2002–3915, presented at the 38th Joint AIAA/ASME/SAE/ASEE Propulsion Conference, Indianapolis, IN, July 2002.
7. Porter, J.L, and Squyers, R.A. “A Summary/Overview of Ejector Augmentor Theory and Performance,” ATC Report No. R–91100/ 9CR–47A, Vought Corporation Advanced Technology Center, Dallas, Texas, (1979). (a) see fig. 42, page 88, (b) see fig. 11, page 24, (c) see fig. 19, page 55, (d) see fig. 33, page 74.
8. Paxson, D.E., “A General Numerical Model for Wave Rotor Analysis,” NASA TM–105740, July 1992.
9. Brocher, E., and Pinna, G., “Aeroacoustical Phenomena in a Horn Excited by a Hartmann-Sprenger Tube,” Acustica, Vol. 45, No. 3, pp. 180–189, 1980.
10. Mason, R.L., Gunst, R.F., and Hess, J.L., “Statistical Design and Analysis of Experiments: with Applications to Engineering and Science,” Wiley, N.Y. 1989.
11. Seshadri, S., and Demming, S.N., “Box-B Interactive Computer Programs for Using Three- and Four-Factor Box-Behnken Designs in Research, Development, and Manufacturing (version 2.1),” A computer program available from: Statistical Programs, 9941 Rowlett, Suite 6, Houston, TX 77075.
12. Elder, F.K. Jr., and de Haas, N., “Experimental Study of the Formation of a Vortex Ring at the Open End of a Cylindrical Shock Tube,” Journal of Applied Physics, 23, pp. 1065–1069, 1952.
13. Payman, W., and Shepherd, W.C.S., “Explosion waves and shock waves VI. The disturbance produced by bursting diaphragms with compressed air,” Proceedings of the Royal Society (London), Vol. A186, pp. 293–321, 1946.
14. Lamb, Sir H., “Hydrodynamics,” Dover, N.Y., 1932.
15. Sallet, D.W., and Widmayer, R.S., “An Experimental Investigation of Laminar and Turbulent Vortex Rings in Air,” Z. Flugwiss, 22, No. 6, pp. 207–215, 1974.
16. Shariff, K., and Leonard, A., “Vortex Rings,” Annu. Rev. Fluid Mech., 24, pp. 235–279, 1992.
17. Gharib, M., Rambod, E., and Shariff, K., “A universal time scale for vortex ring formation,” J. Fluid Mech., 360, pp. 121–149, 1998.

Table 1.—Set of runs performed

Run No.	Diameter (D), in.	Length (L), in.	Nose Radius (R), in.	Optimum (X), in.	α	β	$(1+\beta)^{(\gamma-1)/\gamma}$
1	2.2	3.125	0.5	1.0	1.155		
2	2.2	7.125	0.25	1.0	1.160	0.897	1.20
3	2.2	7.625	0.75	1.0	1.155		
4	2.2	12.375	0.5	0.75	1.092		
5	3	2.875	0.25	2.5	1.264		
6	3	3.375	0.75	2.5	1.275		
7	3	7.375	0.5	2.5	1.330		
8	3	7.375	0.5	3.0	1.325	1.895	1.35
9	3	7.375	0.5	3.0	1.308		
10	3	12.125	0.25	2.0	1.255		
11	3	12.625	0.75	2.0	1.267		
12	6	3.125	0.5	3.0	1.034		
13	6	7.125	0.25	4.0	1.075		
14	6	7.625	0.75	4.0	1.085		
15	6	12.375	0.5	5.0	1.139		
16	4	3.125	0.5	3.0	1.118		
17	4	7.125	0.25	3.5	1.206		
18	4	7.625	0.75	2.5	1.226		
19	4	12.375	0.5	2.5	1.266		
20	2.2	16.5	0.25	1.0	1.094		
21	2.2	17	0.75	0.9	1.106		
22	3	16.5	0.25	2.5	1.285		
23	3	17	0.75	2.3	1.298		
24	4	17	0.75	1.75	1.275		
25	6	16.5	0.25	3.7	1.179		
26	6	17	0.75	3.5	1.251		
27	3	10.75	See fig. 2(b)	2.5	1.288		
28	3	9.75	See fig. 2(b)	2.5	1.275		
29	3	8.5	See fig. 2(b)	3.0	1.324		
30	3	8.0	See fig. 2(b)	2.5	1.309		
31	3	7.25	See fig. 2(b)	2.8	1.310		
32	3	6.25	See fig. 2(b)	2.5	1.300		

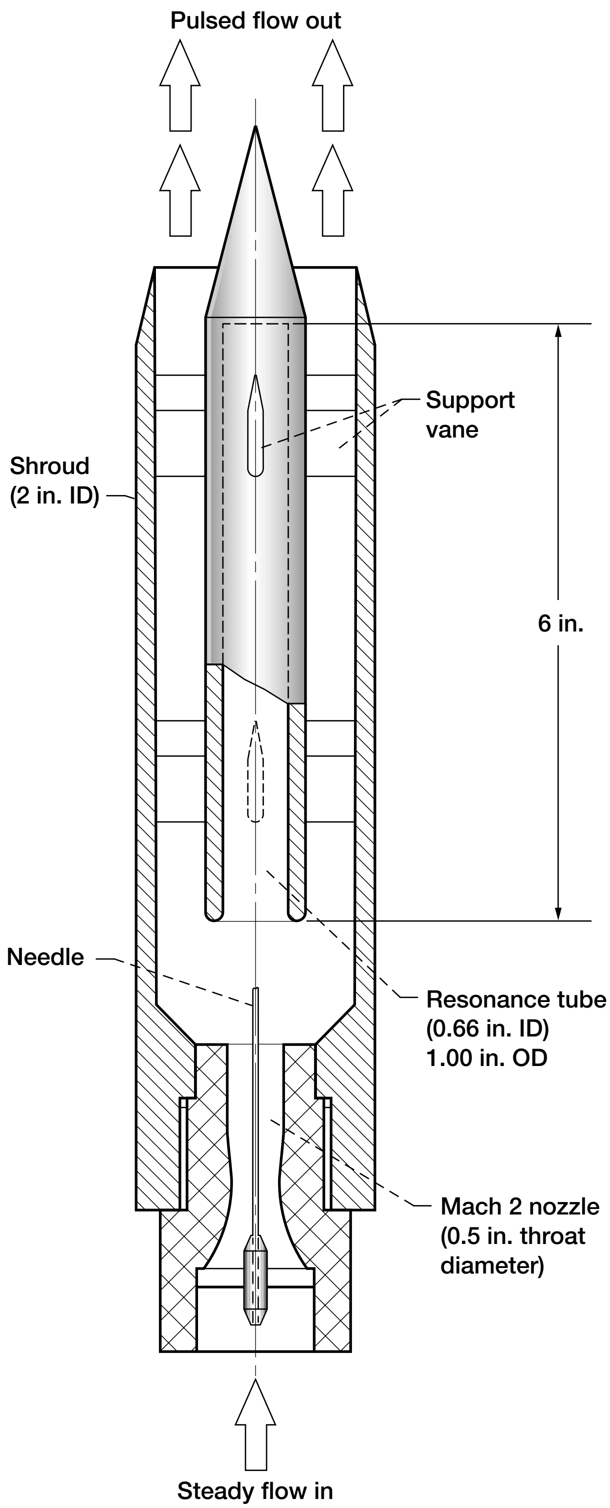

Figure 1.—Drawing of the shrouded Hartmann-Sprenger tube.

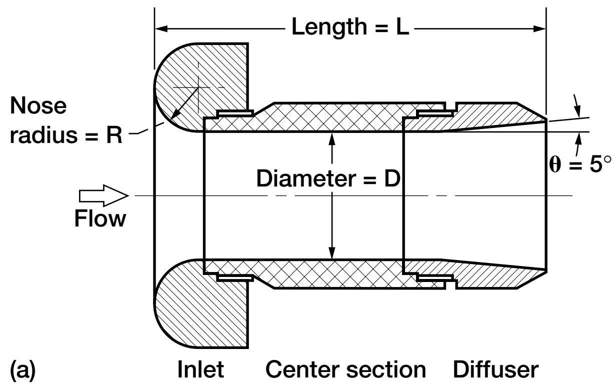

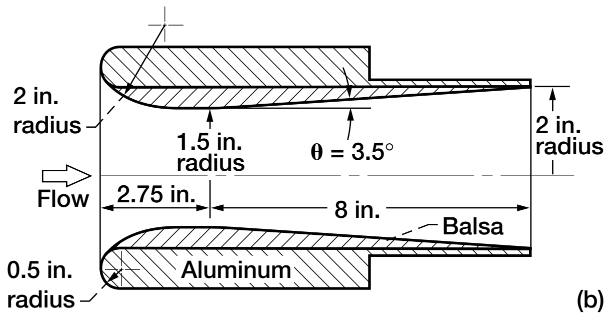

Figure 2.—Drawings of (a) the set of ejectors for the Box-Behnken experiment, and, (b) the contoured ejector.

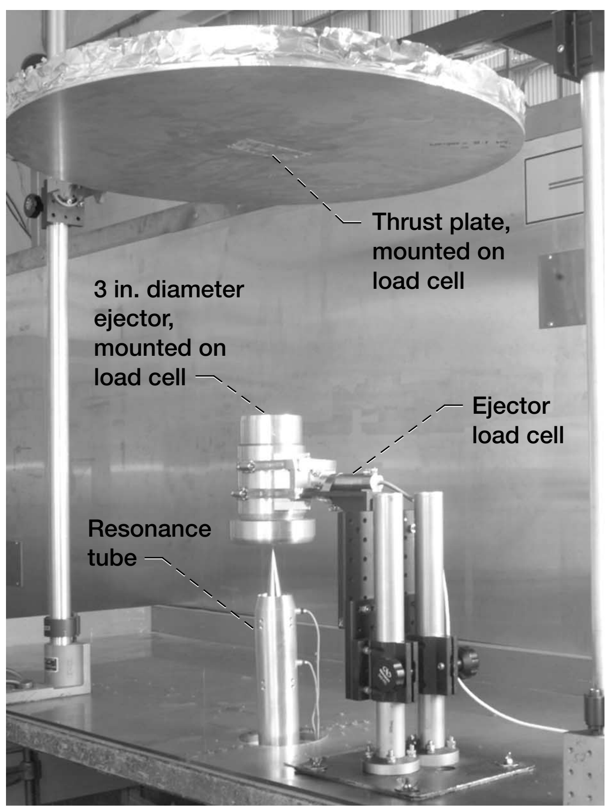

Figure 3.—Photograph of the apparatus.

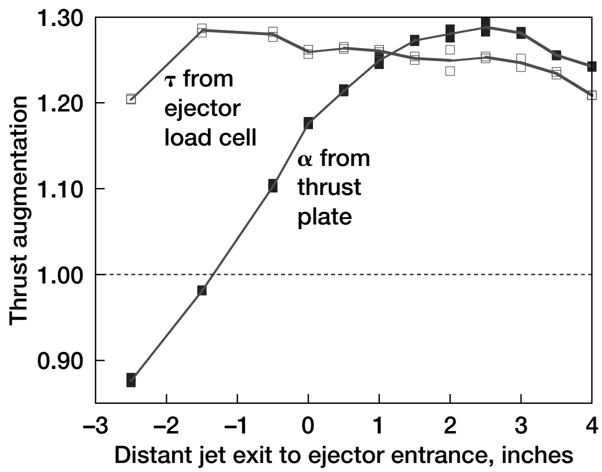

Figure 4.—Plot of thrust augmentation versus the distance between the pulsed jet exit, and the ejector entrance.

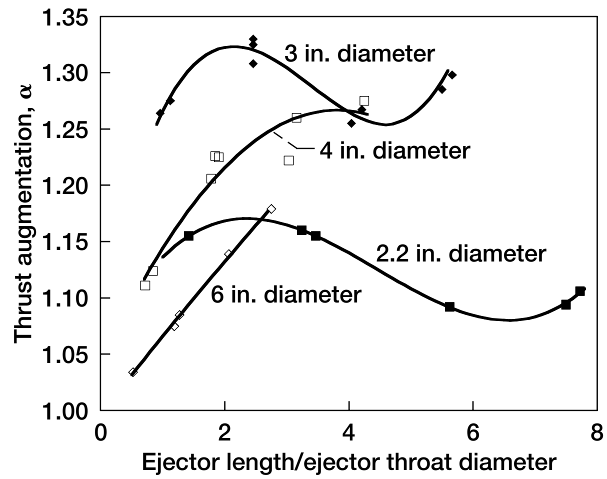

Figure 6.—Thrust augmentation versus ejector length for increased length ejectors.

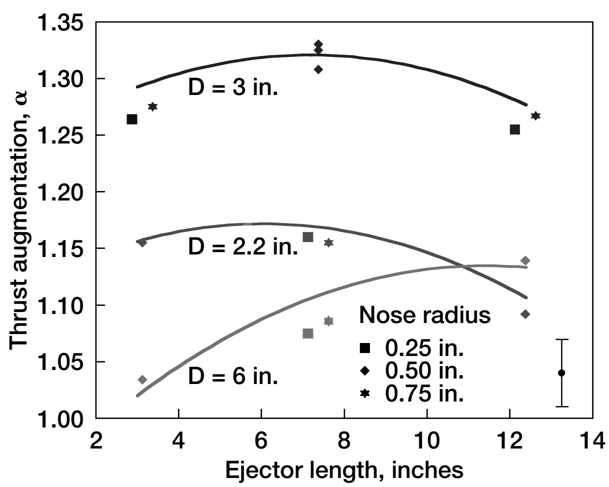

Figure 5.—Results of the initial Box-Behnken experiment. Thrust augmentation versus ejector length.

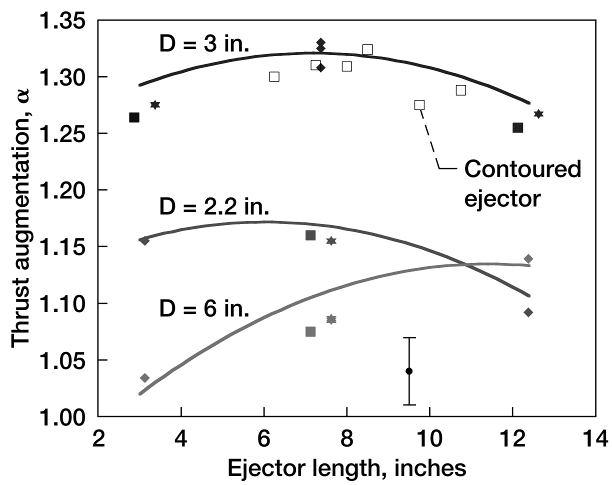

Figure 7.—Thrust augmentation versus length for the contoured ejector of figure 2(b).

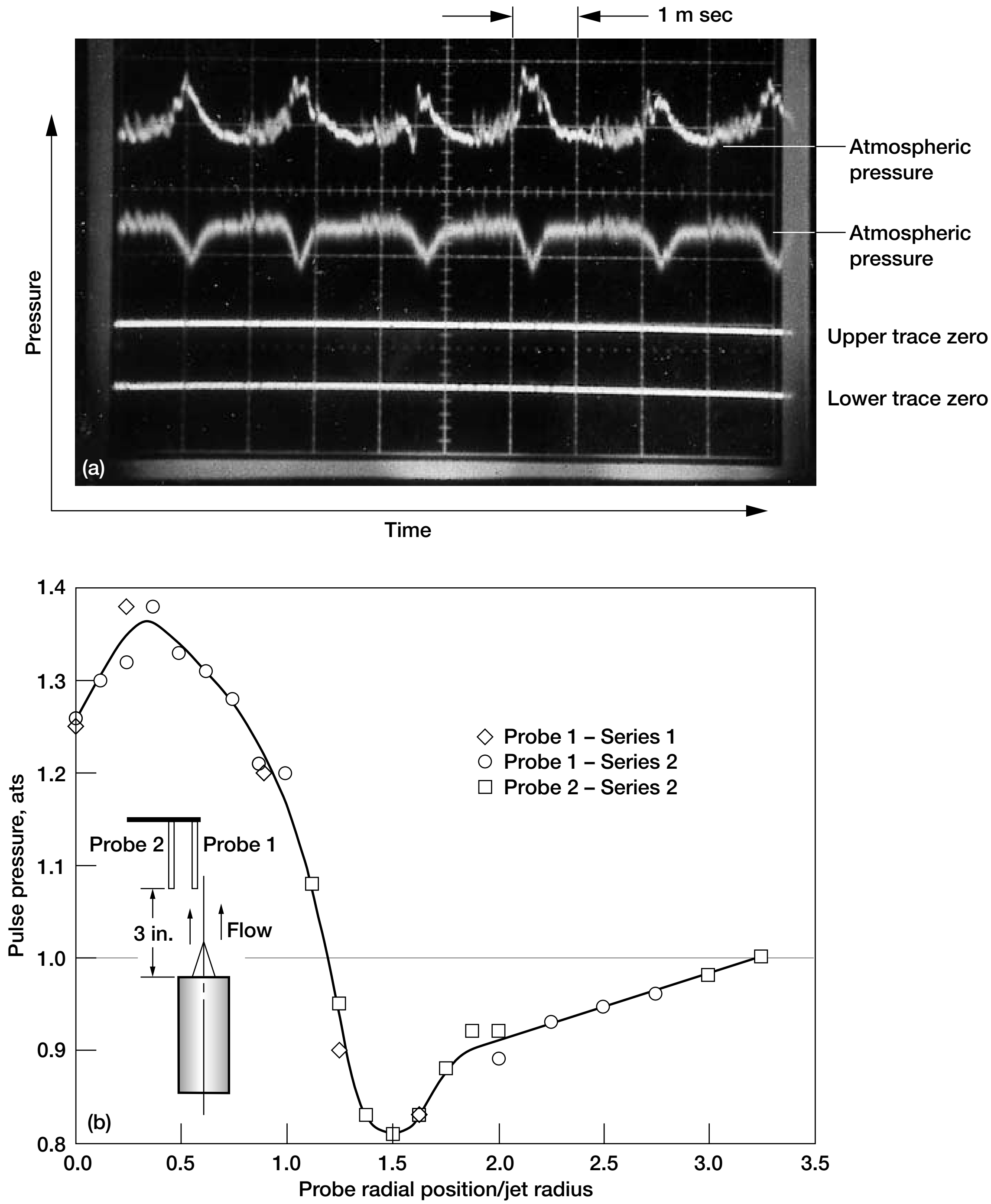

Figure 8.—(a) Oscillogram of pressure measurements in the flow from the resonance tube. The upper trace is taken at radius of 0.5 inches, the lower trace at a radius of 1.5 inches. (b) Jet pressure at maximum pulse excursion versus radial position in the jet.

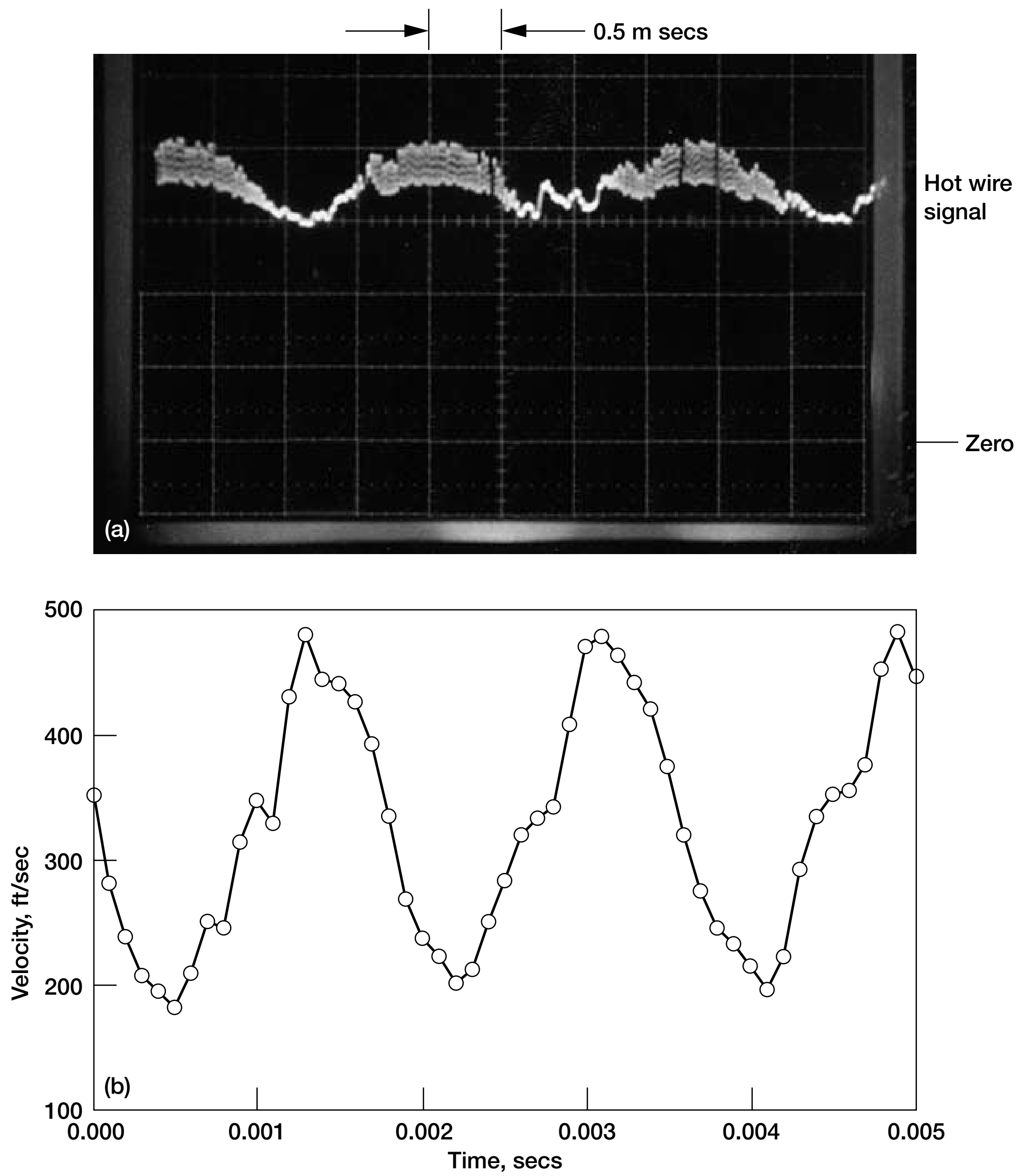

Figure 9.—(a) Signal from the hot-wire situated on the jet axis. (b) The velocity derived from the hot-wire signal.

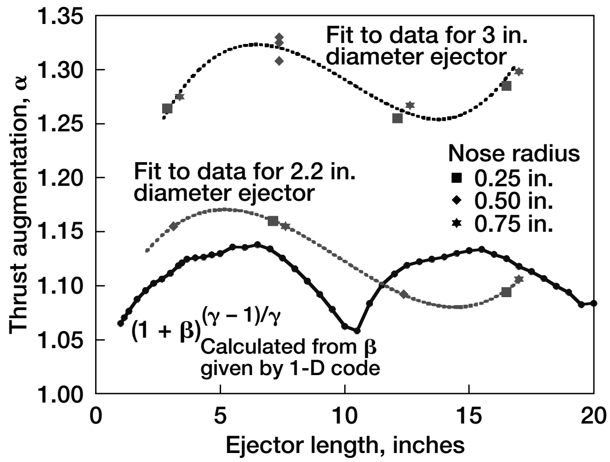

Figure 10.—Thrust augmentation versus ejector length for the 2.2 inch and 3 inch diameter ejectors, compared wih calculated values using the one-dimensional CFD code.

REPORT DOCUMENTATION PAGE

Form Approved
OMB No. 0704-0188

1. AGENCY USE ONLY (*Leave blank*)	2. REPORT DATE	3. REPORT TYPE AND DATES COVERED
	July 2002	Technical Memorandum

4. TITLE AND SUBTITLE

Unsteady Ejector Performance: An Experimental Investigation Using a Resonance Tube Driver

5. FUNDING NUMBERS

WU–708–48–13–00

6. AUTHOR(S)

Jack Wilson and Daniel E. Paxson

7. PERFORMING ORGANIZATION NAME(S) AND ADDRESS(ES)

National Aeronautics and Space Administration
John H. Glenn Research Center at Lewis Field
Cleveland, Ohio 44135–3191

8. PERFORMING ORGANIZATION REPORT NUMBER

E–13239

9. SPONSORING/MONITORING AGENCY NAME(S) AND ADDRESS(ES)

National Aeronautics and Space Administration
Washington, DC 20546–0001

10. SPONSORING/MONITORING AGENCY REPORT NUMBER

NASA TM—2002-211474
AIAA–2002–3632

11. SUPPLEMENTARY NOTES

Prepared for the 38th Joint Propulsion Conference and Exhibit cosponsored by AIAA, ASME, SAE, and ASEE, Indianapolis, Indiana, July 7–10, 2002. Jack Wilson, QSS Group, Inc., Cleveland, Ohio, and Daniel E. Paxson, NASA Glenn Research Center. Responsible person, Jack Wilson, organization code 5810, 216–977–1204.

12a. DISTRIBUTION/AVAILABILITY STATEMENT

Unclassified - Unlimited
Subject Categories: 02 and 07 Distribution: Nonstandard

Available electronically at http://gltrs.grc.nasa.gov/GLTRS

This publication is available from the NASA Center for AeroSpace Information, 301–621–0390.

12b. DISTRIBUTION CODE

13. ABSTRACT *(Maximum 200 words)*

A statistically designed experiment to characterize thrust augmentation for unsteady ejectors has been conducted at the NASA Glenn Research Center. The variable parameters included ejector diameter, length, and nose radius. The pulsed jet driving the ejectors was produced by a shrouded resonance (or Hartmann-Sprenger) tube. In contrast to steady ejectors, an optimum ejector diameter was found, which coincided with the diameter of the vortex ring created at the pulsed jet exit. Measurements of ejector exit velocity using a hot-wire permitted evaluation of the mass augmentation ratio, which was found to correlate to thrust augmentation following a formula derived for steady ejectors.

14. SUBJECT TERMS

Ejectors; Thrust augmentation

15. NUMBER OF PAGES

20

16. PRICE CODE

17. SECURITY CLASSIFICATION OF REPORT	18. SECURITY CLASSIFICATION OF THIS PAGE	19. SECURITY CLASSIFICATION OF ABSTRACT	20. LIMITATION OF ABSTRACT
Unclassified	Unclassified	Unclassified	